

On the importance of optical phonons to thermal conductivity in nanostructures

Zhiting Tian, Keivan Esfarjani, Junichiro Shiomi, Asegun S. Henry, and Gang Chen

Citation: [Applied Physics Letters](#) **99**, 053122 (2011); doi: 10.1063/1.3615709

View online: <http://dx.doi.org/10.1063/1.3615709>

View Table of Contents: <http://scitation.aip.org/content/aip/journal/apl/99/5?ver=pdfcov>

Published by the [AIP Publishing](#)

Articles you may be interested in

[Thermal transport in crystalline Si/Ge nano-composites: Atomistic simulations and microscopic models](#)

Appl. Phys. Lett. **100**, 091903 (2012); 10.1063/1.3688943

[Phonon thermal conductivity in silicon nanowires: The effects of surface roughness at low temperatures](#)

J. Appl. Phys. **111**, 044304 (2012); 10.1063/1.3684973

[Thermal conductivity of silicon nanowire by nonequilibrium molecular dynamics simulations](#)

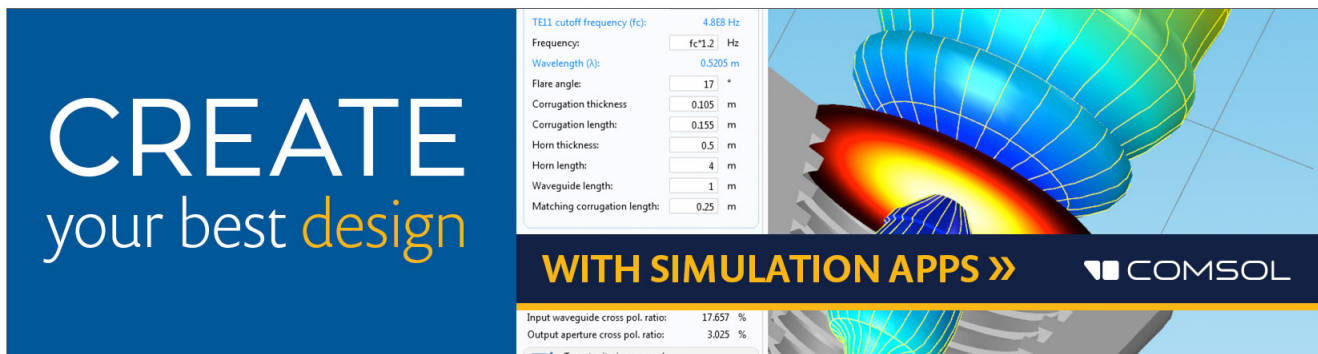
J. Appl. Phys. **105**, 014316 (2009); 10.1063/1.3063692

[Monte Carlo simulation of phonon confinement in silicon nanostructures: Application to the determination of the thermal conductivity of silicon nanowires](#)

Appl. Phys. Lett. **89**, 103104 (2006); 10.1063/1.2345598


[Raman scattering on silicon nanowires: The thermal conductivity of the environment determines the optical phonon frequency](#)

Appl. Phys. Lett. **88**, 233114 (2006); 10.1063/1.2210292



CREATE
your best design

TE11 cutoff frequency (fc): 4.868 Hz
Frequency: Hz
Wavelength (λ): 0.5205 m
Flare angle: °
Corrugation thickness: m
Corrugation length: m
Horn thickness: m
Horn length: m
Waveguide length: m
Matching corrugation length: m

WITH SIMULATION APPS >> 

Input waveguide cross pol. ratio: 17.657 %
Output aperture cross pol. ratio: 3.025 %
 Target criterion: passed

On the importance of optical phonons to thermal conductivity in nanostructures

Zhiting Tian, Keivan Esfarjani, Junichiro Shiomi, Asegun S. Henry, and Gang Chen^{a)}
*Department of Mechanical Engineering, Massachusetts Institute of Technology, Cambridge,
 Massachusetts 02139, USA*

(Received 19 April 2011; accepted 1 July 2011; published online 5 August 2011)

The contribution of optical phonons to thermal conductivity has typically been ignored. However, when the system size decreases to the nanoscale regime, optical phonons are no longer negligible. In this study, the contributions of different phonon polarizations to the thermal conductivity of silicon are discussed based on the phonon lifetimes extracted from a first principles approach. The results indicate that around room temperature, optical phonons can contribute over 20% to the thermal conductivity of nanostructures as compared to 5% in bulk materials. In addition, the temperature and size dependence of the contributions from acoustic and optical phonons are fully explored. © 2011 American Institute of Physics. [doi:10.1063/1.3615709]

It is generally understood that optical phonon contributions to thermal conductivity are small and negligible in bulk materials because of their short lifetimes and low group velocities. Several recent theoretical efforts^{1–4} that fully detail the spectral phonon transport properties of bulk silicon (Si) all concluded that the contribution of optical phonons is around 5% at room temperature, regardless of the method used. Although the contribution of optical phonons is small, Ward and Broido⁵ highlighted the importance of optical phonons in the sense that they provide an important scattering channel for acoustic phonons, and therefore, if removed from the system, would lead to a dramatic increase in the thermal conductivity.

When the system size decreases, however, the contributions of optical phonons to heat conduction become increasingly important. While acoustic phonons are strongly scattered at boundaries and interfaces, optical phonons have short mean free paths (MFPs) and are scattered much more strongly inside the nanostructures than at the boundaries. Such difference in scattering leads to a rebalance of the relative importance of optical phonons and acoustic phonons to the thermal conductivity of nanostructures. In this letter, we examine this shift using Si as a test case, because several puzzling experimental results for Si nanowires^{6–9} have yet to be explained satisfactorily, despite several theoretical and computational studies.^{10–16} Based on first principles calculations, we first examine the cumulative contributions to thermal conductivity in bulk Si by phonons with different MFPs and polarizations, namely, longitudinal acoustic (LA), transverse acoustic (TA), longitudinal optical (LO), and transverse optical (TO). We then model the thermal conductivity of Si nanowires based on the spectral properties in bulk Si and evaluate the contributions of optical phonons as a function of nanowire diameter over a wide temperature range. Our modeling results show that around room temperature, optical phonon contributions can increase to 18% when the nanowire diameter is reduced to 20 nm.

^{a)}Author to whom correspondence should be addressed. Electronic mail: gchen2@mit.edu.

The detailed methodology and calculation procedures for bulk Si are presented elsewhere.^{17,18} In short, electronic structure calculations based on density functional theory were applied to extract interatomic force constants via the direct displacement method.¹⁷ The cubic anharmonic force constants lead to three-phonon lifetimes. The phonon lifetimes $\tau_{k,p}$ due to the normal and umklapp three-phonon scattering processes have been calculated for each polarization p and each k point sampled in the first Brillouin zone based on the scattering rate determined from application of Fermi's golden rule. The thermal conductivity is then computed from the relaxation time approximation using the well-known formula

$$\kappa = \frac{1}{3\Omega N_k} \sum_{k,p} v_{k,p}^2 \tau_{k,p} \hbar \omega_{k,p} \frac{\partial n_{k,p}}{\partial T}, \quad (1)$$

where Ω is the volume of the unit cell and $n_{k,p}$ is the Bose-Einstein distribution. The phonon MFP for each mode is defined as

$$\Lambda_{k,p} = v_{k,p} \tau_{k,p}. \quad (2)$$

By sorting the thermal conductivity contribution of each mode according to increasing MFPs,^{1,19} the polarization dependent and total cumulative thermal conductivity can be determined by Eqs. 3(a) and 3(b), respectively, as follows:

$$\kappa_p(\Lambda) = \frac{1}{3\Omega N_k} \sum_k^{\Lambda_{k,p} < \Lambda} v_{k,p} \Lambda_{k,p} \hbar \omega_{k,p} \frac{\partial n_{k,p}}{\partial T}, \quad (3a)$$

$$\kappa(\Lambda) = \sum_p \kappa_p(\Lambda). \quad (3b)$$

As the system size decreases, it is often found that a large thermal conductivity reduction occurs as the nanometer regime is approached.^{19–26} Past studies suggest that this reduction is due mainly to boundary scattering. The effective phonon lifetimes including boundary scattering can be

estimated by adding the scattering rates due to anharmonic and boundary processes

$$\frac{1}{\tau_{k,p}} = \frac{1}{\tau_{k,p}^{p-p}} + \frac{1}{\tau_{k,p}^B}, \quad (4)$$

where for nanowires with diameter d , the Casimir limit²⁷ gives

$$\frac{1}{\tau_{k,p}^B} = \frac{v_{k,p}}{d}, \quad (5)$$

which assumes purely diffuse scattering at the boundary. Alternatively, by solving Boltzmann's equation for an infinite wire, Sondheimer also arrived at a similar result, and generalized it to the case of boundaries with scattering continuously going from specular to diffuse.²⁸

The detailed cumulative contributions to thermal conductivity by phonons of different MFPs and polarizations at 277 K are shown in Figure 1. Note the slope change in thermal conductivity when the phonon MFPs are ~ 30 nm. Inset (a) in Figure 1 shows that this sharp increase is due to the rapid growth in contributions from the TA phonons. Contributions to the total thermal conductivity for phonons with a MFP less than ~ 30 nm are mainly due to LA and optical phonons. Although TO phonons have very short MFPs (less than 9 nm), they are dominant contributors (inset (b)) to thermal conductivity in this MFP range, due to their large density of states (DOS).

Figure 1 also leads to additional insights on the contributions of acoustic modes to the thermal conductivity. Below 45 nm, LA modes contribute more to the thermal conductivity than TA modes. These small MFP modes correspond to phonons near the first Brillouin zone edge where the group velocities of TA modes are lower than those of LA modes. The sharp increase of TA2 accumulation between 40 nm and 100 nm is due to larger DOS of TA2 modes.

Considering the properties of different polarizations in bulk Si presented above, we investigate how the contributions change in the context of nanowires. To validate our model, we first compare the thermal conductivities of nano-

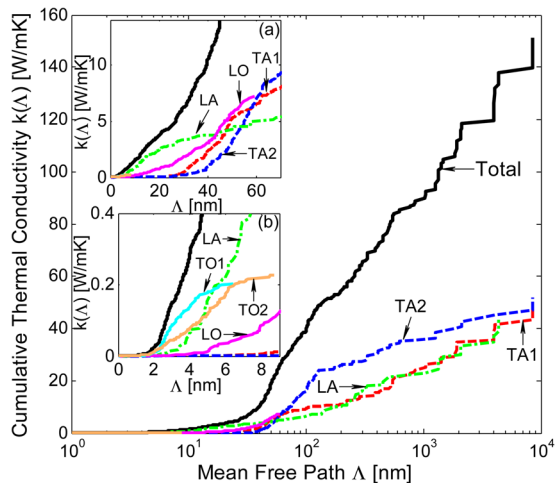


FIG. 1. (Color online) Cumulative thermal conductivity with respect to MFPs at 277 K from the $18 \times 18 \times 18$ k-mesh data; Inset (a)-Inset (b) Zoomed-in figures for MFP range of 0-70 nm and 0-9 nm, respectively.

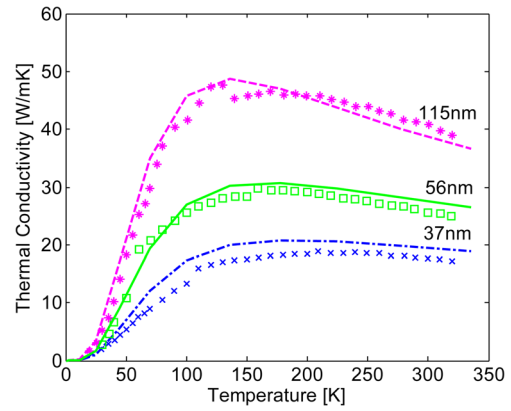


FIG. 2. (Color online) Thermal conductivity of silicon nanowires for $d = 37$ nm, 56 nm, and 115 nm, lines: calculated results; crosses: experimental results (see Ref. 6).

wires with experimental results. To best represent the experimental sample, we add the scattering rate as below

$$\frac{1}{\tau_{k,p}} = \frac{1}{\tau_{k,p}^{p-p}} + \frac{1}{\tau_{k,p}^B} + \frac{1}{\tau_{k,p}^i} \quad \text{and} \quad \frac{1}{\tau_{k,p}^i} = A\omega_{k,p}^4, \quad (6)$$

where $A = 1.32 \times 10^{-44} \text{s}^3$ is analytically determined from the isotope concentration and given in Ref. 29. Without any fitting parameters, we have obtained decent agreement with experimental data⁶ for $d = 115$ nm, 56 nm, and 37 nm as shown in Figure 2. The good representation supports the following discussions based on the boundary scattering effect. We do not include the nanowire of 22 nm since we could not

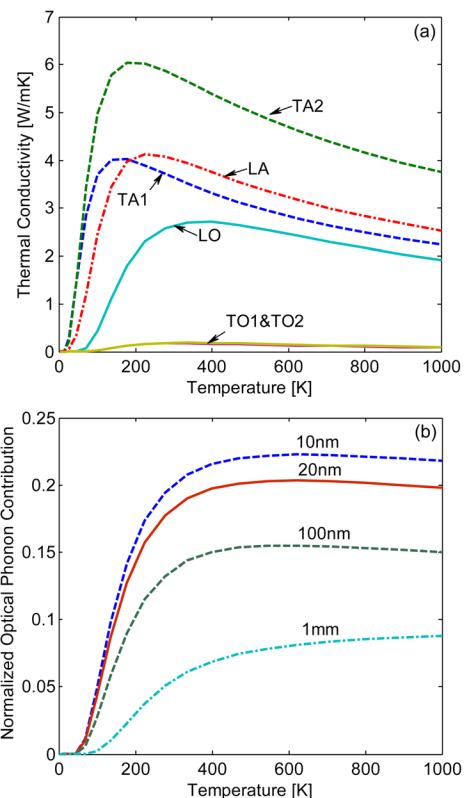


FIG. 3. (Color online) Thermal conductivity from different polarizations versus temperature for $d = 20$ nm; (b) normalized optical phonon contributions to the total thermal conductivity versus temperature for $d = 10$ nm, 20 nm, 100 nm, and 1 mm.

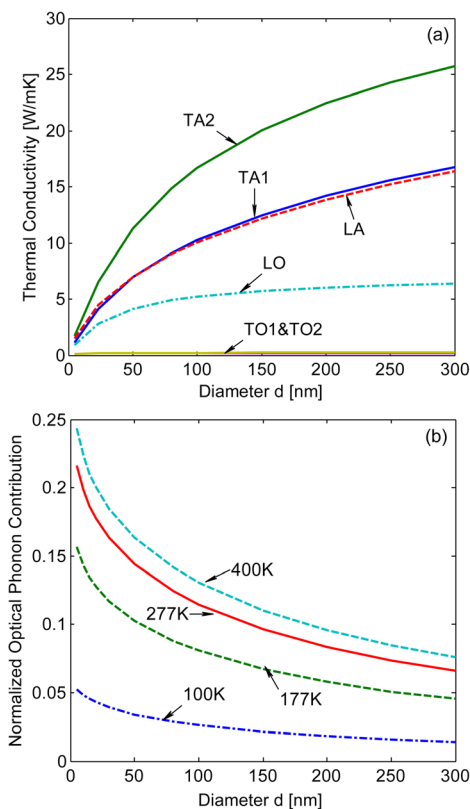


FIG. 4. (Color online) (a) Thermal conductivity from different polarizations versus diameters at 277 K and (b) normalized optical phonon contributions to the total thermal conductivity vs. diameters at 100 K, 177 K, 277 K, and 400 K.

explain the experimental results after taking into account the optical phonon contributions.

The temperature dependence of relative phonon contributions from different polarizations is shown in Figure 3(a) for the $d = 20$ nm nanowire. At temperatures below 100 K, the acoustic thermal conductivity exhibits T^3 dependence, the same as the temperature dependence of the specific heat, due to the dominance of boundary scattering. Two TA modes grow more rapidly than LA modes as the specific heat of TA modes rises more rapidly due to their lower frequency and higher DOS. LO modes' contributions are noteworthy over most of the temperature range considered. TO modes, however, are negligible for this diameter.

Adding LO and TO modes together, the normalized optical phonon contributions are shown in Figure 3(b) for different nanowire diameters. As diameter decreases, the optical phonon contributions relative to acoustic phonons become larger as expected. Between 0 K and 300 K, the optical phonon contributions increase due to the increase in their specific heat.

Figure 4(a) depicts the thermal conductivities from different polarizations for Si nanowires of different diameters, varying from 5 nm to 300 nm, at 277 K. Acoustic phonon contributions increase with increasing diameter in the plotted diameter range (5-300 nm), while the optical phonon contributions saturate around 100 nm due to their lower MFP values arising from three phonon scattering processes. The normalized contributions with the total thermal conductiv-

ities at different temperatures are shown in Figure 4(b). At 277 K, the optical phonon contributions grow from below 10% to 21% when d decreases from 300 nm to 5 nm. It suggests that optical phonons can have significant impact on thermal conductivity in nanostructures, especially at temperatures on the order of the Debye temperature or higher.

In summary, we have used relaxation times determined from first principles derived force constants to calculate the thermal conductivity of bulk Si and Si nanowires. Detailed analysis of the respective contributions shows that optical phonons comprise up to 20% of the total thermal conductivity in Si nanowires around room temperature, despite conventional wisdom, which suggests that their contributions are usually negligible. This finding brings to light the importance of optical phonon contributions to heat conduction in nanostructures. Although Si is taken as the model material, we expect that similar behavior should exist in many other materials.

This material is based upon work supported as part of the "Solid State Solar-Thermal Energy Conversion Center (S3TEC)," an Energy Frontier Research Center funded by the U.S. Department of Energy, Office of Science, Office of Basic Energy Sciences under Award Number: DE-SC0001299/DE-FG02-09ER46577.

- ¹A. S. Henry and G. Chen, *J. Comput. Theor. Nanosci.* **5**, 141 (2008).
- ²D. A. Broido, M. Malorny, G. Birner, N. Mingo, and D. A. Stewart, *Appl. Phys. Lett.* **91**, 231922 (2007).
- ³L. Sun and J. Y. Murthy, in *ASME Conference Proceedings*, San Francisco, CA, USA, 17–22 July 2005.
- ⁴D. P. Sellan, J. E. Turney, A. J. H. McGaughey, and C.H. Amon, *J Appl. Phys.* **108**, 113524 (2010).
- ⁵A. Ward and D. A. Broido, *Phys. Rev. B* **81**, 085205 (2010).
- ⁶D. Li, Y. Wu, P. Kim, L. Shi, P. Yang, and A. Majumdar, *Appl. Phys. Lett.* **83**, 2934 (2003).
- ⁷A. I. Boukai, Y. Bunimovich, J. Tahir-Kheli, J.-K. Yu, W. A. Goddard, and J. R. Heath, *Nature* **451**, 168 (2008).
- ⁸A. I. Hochbaum, R. Chen, R. D. Delgado, W. Liang, E. C. Garnett, M. Najarian, A. Majumdar, and P. Yang, *Nature* **451**, 163 (2008).
- ⁹K. Hippalgaonkar, B. Huang, R. Chen, K. Sawyer, P. Ercius, and A. Majumdar, *Nano Lett.* **10**, 4341 (2010).
- ¹⁰S. G. Volz and G. Chen, *Appl. Phys. Lett.* **75**, 2056 (1999).
- ¹¹N. Mingo, L. Yang, D. Li, and A. Majumdar, *Nano Lett.* **3**, 1713 (2003).
- ¹²Y. Chen, D. Li, J. R. Lukes, and A. Majumdar, *J. Heat Transf.* **127**, 1129 (2005).
- ¹³P. G. Murphy and J. E. Moore, *Phys. Rev. B* **76**, 155313 (2007).
- ¹⁴I. Ponomareva, D. Srivastava, and M. Menon, *Nano Lett.* **7**, 1155 (2007).
- ¹⁵R. Chen, A. I. Hochbaum, P. Murphy, J. Moore, P. Yang, and A. Majumdar, *Phys. Rev. Lett.* **101**, 105501 (2008).
- ¹⁶D. Donadio and G. Galli, *Phys. Rev. Lett.* **102**, 195901 (2009).
- ¹⁷K. Esfarjani and H. T. Stokes, *Phys. Rev. B* **77**, 144112 (2008).
- ¹⁸K. Esfarjani, G. Chen, and H. T. Stokes, *Phys. Rev. B*, arXiv:1107.5288v1 [cond-mat.mtrl-sci] (to be published).
- ¹⁹C. Dames and G. Chen, in *CRC Handbook*, edited by M. Rowe (Taylor & Francis, Boca Raton, FL, 2006).
- ²⁰G. Chen, T. Zeng, T. Borca-Tasciuc, and D. Song, *Mater. Sci. Eng. A* **292**, 155 (2000).
- ²¹D. G. Cahill, W. K. Ford, K. E. Goodson, G. D. Mahan, A. Majumdar, H. J. Maris, R. Merlin, and S. R. Phillpot, *J. Appl. Phys.* **93**, 793 (2003).
- ²²C. Dames and G. Chen, *J. Appl. Phys.* **95**, 682 (2004).
- ²³L. H. Liang and B. Li, *Phys. Rev. B* **73**, 153303 (2006).
- ²⁴S. K. Bux, R. G. Blair, P. K. Gogna, H. Lee, G. Chen, M. S. Dresselhaus, R. B. Kaner, and J.-P. Fleurial, *Adv. Funct. Mater.* **19**, 1 (2009).
- ²⁵P. Yang, R. Yan, and M. Fardy, *Nano Lett.* **10**, 1529 (2010).
- ²⁶J. Chen, G. Zhang, and B. Li, *Nano Lett.* **10**, 3978 (2010).
- ²⁷H. B. G. Casimir, *Physica (Amsterdam)* **6**, 495 (1938).
- ²⁸E. H. Sondheimer, *Adv. Phys.* **1**, 1 (1952).
- ²⁹M. G. Holland, *Phys. Rev.* **132**, 2461 (1963).